Journal of Applied Electrochemistry **29**: 765–771, 1999.

Anodically deposited manganese-molybdenum oxide anodes with high selectivity for evolving oxygen in electrolysis of seawater

K. FUJIMURA[1], K. IZUMIYA[2], A. KAWASHIMA[1], E. AKIYAMA[1], H. HABAZAKI[1], N. KUMAGAI[3] and K. HASHIMOTO[1]
[1]*Institute for Materials Research, Tohoku University, Sendai, 980-8577 Japan;*
[2]*Mitsui Engineering & Shipbuilding Co., Ltd. Ichihara, Chiba 290-8601, Japan;*
[3]*Daiki Engineering Company, Ltd, 11 Shintoyofuta, Kashiwa, Chiba 277-8515, Japan*

Received 16 June 1998; accepted in revised form 24 November 1998

Key words: anodic deposition, manganese-molybdenum oxide electrode, oxygen evolution, seawater electrolysis

Abstract

Manganese-molybdenum oxide electrodes were prepared by anodic deposition on an IrO_2-coated titanium substrate at a constant current density of 600 A m^{-2} from baths containing 0.2 M $MnSO_4$ and 0–0.1 M Na_2MoO_4 at 90 °C and pH 0.5. These electrodes were characterised for oxygen evolution in the electrolysis at 1,000 A m^{-2} in 0.5 M NaCl solution at 30 °C and pH 8 or 12. The most active and stable oxygen evolving anode exhibited 100% efficiency for oxygen evolution, and an efficiency of 98.5% for over 1,500 h at pH 12 and of 96.5% for over 2,800 h at pH 8 of continuous electrolysis. X-ray diffraction measurement and XPS analysis indicated that the deposits consist of a nanocrystalline single γ-MnO_2 type phase, and manganese and molybdenum in the deposits are in the Mn^{4+} and Mo^{6+} states. The electrochemical studies showed that the manganese-molybdenum oxide electrodes drastically reduced the electrocatalytic activity for chlorine evolution to the undetectable level, resulting in 100% efficiency for oxygen evolution, although the addition of molybdenum slightly increased the oxygen overpotential.

1. Introduction

With the aim of preventing global warming and supplying abundant renewable energy to energy consuming districts some of the present authors are proposing global CO_2 recycling [1–6]. The recycling consists of generation of electricity by solar panels in deserts, H_2 production by seawater electrolysis and CH_4 production by the reaction of H_2 with CO_2 at coastal locations close to the deserts, and CH_4 combustion and CO_2 recovery in the energy consuming districts.

Anodes for oxygen evolution by seawater electrolysis must not evolve toxic chlorine and must have high efficiency and long durability. It is well known, however, that most of the conventional anodes for seawater electrolysis have been tailored to produce chlorine. The existence of commercial seawater electrolysers which efficiently produce hypochlorite solution from anodically generated chlorine [7–9] confirms the predominance of the chlorine evolution. Only manganese oxide coated electrodes are known to produce oxygen with high efficiency in seawater electrolysis [10–16]. However, the oxygen evolution efficiency is not sufficiently high to avoid chlorine evolution.

In previous work, we investigated the oxygen evolution efficiency of thermally decomposed manganese oxides with various cations coated on to IrO_2-coated titanium substrate [17–19]. The oxygen evolution efficiency of the α-Mn_2O_3 anode was about 71% at 200 A m^{-2} in 0.5 M NaCl solution at 30 °C and pH 8. When small amounts of various metallic salts were added to manganese salts α-Mn_2O_3-type oxides were always formed. Small additions of molybdenum and tungsten were effective in enhancing the oxygen evolution efficiency and these electrodes showed an efficiency of about 91% [17]. We have also investigated the oxygen evolution efficiency of anodically deposited manganese-tungsten oxides and reported that they consist of a single orthorhombic γ-MnO_2 type phase and exhibit an efficiency of 99.6% [20]. It is expected that addition of

molybdenum to anodically deposited manganese oxide will enhance the efficiency for oxygen evolution in the seawater electrolysis.

In practical electrolysis cells it is necessary to avoid mixing oxygen and hydrogen gases evolved from the anode and cathode, respectively. If a membrane cell is used, currently used in chlor-alkali industry, the pH of the anolyte will decrease but that of the catholyte will increase. As the anolyte becomes more acidic, the thermodynamic potential for oxygen evolution becomes higher and chlorine evolution, which is independent of pH, is increasingly favored. Furthermore, manganese oxide electrodes are known to be unstable in acidic solution. Izumiya [21] has proposed a new seawater electrolysis cell in which neutral seawater is introduced firstly to the cathode chamber and subsequently to the anode chamber. Seawater becomes alkaline due to hydrogen evolution but is neutralised by oxygen evolution. The seawater at the outlet of the anode chamber must be neutral and returned to the ocean. Preliminary work [21] on electrolysis of a neutral sodium chloride solution has shown that the anolyte inlet pH was about 12, but was 8 at the outlet. In this work electrolytes of pH 8 and 12 were used.

The present work aims to examine the oxygen evolution efficiency of anodically deposited manganese-molybdenum oxide electrodes in the electrolysis of NaCl solutions.

2. Experimental procedure

IrO_2-coated titanium plate and expanded titanium metal were utilised as substrates. Preparation of the substrates has been described in detail elsewhere [17–20]. The intermediate IrO_2 layer is needed to avoid the formation of an insulating titanium oxide layer on titanium in the course of electrolysis of sodium chloride solutions.

Manganese oxide and manganese-molybdenum oxides were anodically deposited on the IrO_2-coated titanium substrates at a constant current density of 600 A m^{-2} from baths containing 0.2 M $MnSO_4$ and 0–0.1 M Na_2MoO_4. Before deposition, the substrates were anodically polarised at 1,000 A m^{-2} for 10 min in 1 M H_2SO_4 to remove the contaminants during IrO_2-coating process and rinsed with distilled water. The deposition times were 10 and 30 min for manganese oxide and manganese-molybdenum oxides, respectively. The Pyrex glass H-type cell was used as an electrolytic cell with separation of anode and cathode compartments. The platinum-coated titanium plate was used as a counter electrode. The pH of the baths was initially adjusted to 0.5 by adding 18 M H_2SO_4 and the temperature of the baths was kept at 90 °C.

The structure of the deposits was examined by X-ray diffraction using Cu Kα radiation. The molybdenum content of the deposits was determined by an electron probe microanalyzer (Shimadzu EPMA-C1). X-ray photoelectron spectroscopy (XPS) by means of a Shimadzu ESCA 850 photoelectron spectrometer with Mg Kα ($h\nu = 1253.6$ eV) excitation was employed for the surface analysis of anodically deposited oxides. The binding energies of electrons were calibrated using methods described elsewhere [22, 23].

Anode performance was examined by galvanostatic and potentiodynamic polarisation in 0.5 M NaCl solutions at 30 °C and pH 8 and 12. A stirred undivided glass cell was used for electrolysis of sodium chloride solutions. A platinum gauze was used as counter electrode for potentiodynamic anodic polarisation. The anodic potentiodynamic polarisation curves were measured from the open-circuit potential to 1.5 V vs SCE at a potential sweep rate of 20 mV min^{-1}. A saturated calomel electrode (SCE) was used as reference. Correction of ohmic drop was made using a Hokuto IR Compensation Instrument for the measurements of potentiodynamic polarisation and a current interruption method for the measurements of galvanostatic polarisation.

The oxygen evolution efficiency was determined from the chlorine evolution efficiency [24]. For the measurements of chlorine evolution efficiency a platinum wire with a small surface area of 0.01 cm^2 was used in order to avoid reduction of hypochlorite ions, formed on the anode, on the counter electrode. The electrolysis was conducted at a constant current density of 1,000 A m^{-2} in 300 ml of 0.5 M NaCl solution until 300 coulombs were passed. The ratio of the solution volume to the nominal specimen surface area was set to 100 cm [20]. The solution analysis was carried out after the measurement of chlorine evolution efficiency by using inductively coupled plasma emission spectroscopy (ICP) (Hitachi HP-2000) and no trace of element such as molybdenum or manganese was found. Therefore, the oxygen evolution efficiency was determined as the difference between the total charge passed and the charge for chlorine evolution. The charge for chlorine evolution during electrolysis was measured by iodimetric titration of chlorine and hypochlorite. Chlorine and hypochlorite converted added iodide into iodine. Iodine was titrated with 0.01 M $Na_2S_2O_3$.

The durability of the electrodes was examined at the current density of 1,000 A m^{-2} in 0.5 M NaCl solution at 30 °C and pH 8 or 12. For the durability test, IrO_2-coated titanium expanded metal was used as the

substrate, because the adhesiveness of the deposits to the expanded metal substrate was found to be high enough compared with plane titanium substrate [20].

3. Results and discussion

With different bath compositions, the molybdenum content and the current efficiency of the deposits varied considerably. Figure 1 shows the change in molybdenum content in manganese oxides anodically deposited at 600 A m^{-2} from 0.2 M $MnSO_4$ at pH 0.5 and 90 °C and the current efficiency for deposition as a function of concentration of Na_2MoO_4 in the baths. In the test range, the molybdenum content increases sharply with a small addition of Na_2MoO_4 into the bath up to 0.02 mol, and eventually tends to be constant at high Na_2MoO_4 contents, the reverse is true for the current efficiency. The concentration of molybdenum of the manganese-molybdenum deposits is significantly high while their current efficiency is much lower compared to the manganese-tungsten deposits [20]; for example, if the cationic % of molybdenum is expressed as mol%, the molybdenum content is about 13 mol% at a current efficiency of about 3.6%, while the tungsten content is about 5.5 mol% at a current efficiency of about 17% for manganese-tungsten oxide anodically deposited at 600 A m^{-2} from 0.2 M $MnSO_4 + 0.02$ M Na_2WO_4 at 90 °C and pH 0.5.

X-ray diffraction patterns of deposits prepared in baths of pH 0.5 containing different concentrations of Na_2MoO_4 are presented in Figure 2. The molybdenum-free deposit consists of γ-MnO_2. All reflections of the manganese-molybdenum oxides are assigned to the γ-MnO_2 phase and no reflections corresponding to molybdenum oxides or molybdenum-containing double oxides are detected. The reflections of IrO_2 from the substrate are seen in the deposits containing 19 and 22 mol% Mo, indicating that thin deposit films are formed at high molybdenum contents due to the remarkably low current efficiency for the deposition. Therefore, all the manganese-molybdenum oxides tested in this study are composed of a single γ-MnO_2 type phase. Diffuse reflections from the molybdenum-containing deposits indicate that the deposit is composed of nanocrystalline grains.

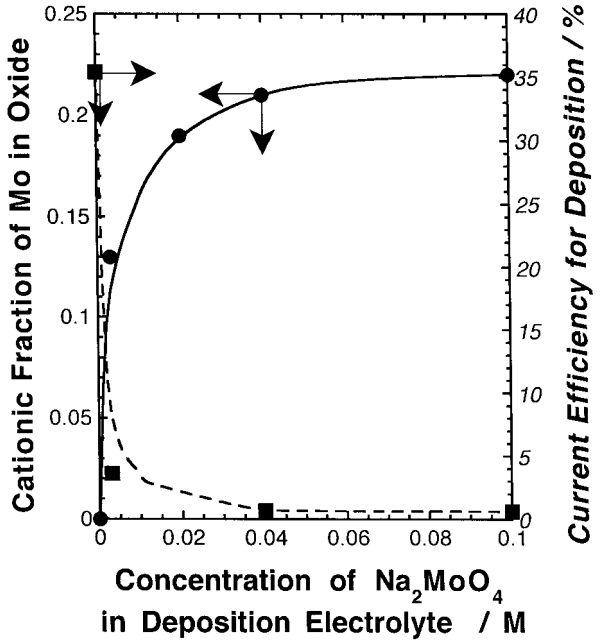

Fig. 1. Change in the concentration of molybdenum (●) in anodically deposited manganese-molybdenum oxides on the IrO_2-coated titanium substrates at 600 A m^{-2} from the baths containing 0.2 M $MnSO_4$ and 0–0.1 M Na_2MoO_4 at pH 0.5 and 90 °C. Current efficiency for the deposition (■) is also shown.

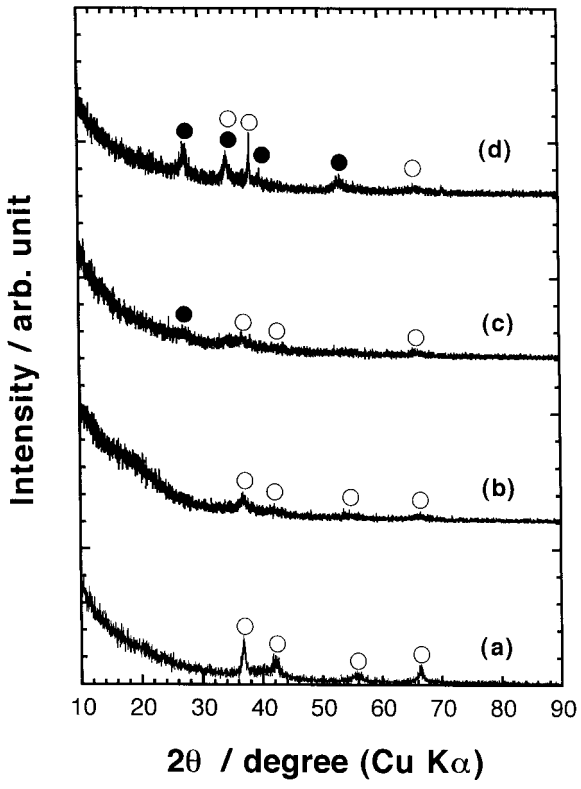

Fig. 2. X-ray diffraction patterns of anodically deposited MnO_2 and $Mn_{1-x}Mo_xO_{2+x}$ on the IrO_2-coated titanium substrates prepared at 600 A m^{-2} from the baths containing 0.2 M $MnSO_4$ and 0–0.1 M Na_2MoO_4 at pH 0.5 and 90 °C. (a) 0 M (x = 0), (b) 0.003 M (x = 0.13), (c) 0.02 M (x = 0.19) and (d) 0.1 M (x = 0.22) Na_2MoO_4. ○: γ-MnO_2, ●: IrO_2.

The XPS spectra of manganese-molybdenum oxides over a wide binding energy region exhibited similar results to those of manganese-tungsten oxides reported previously [20], except for the molybdenum spectrum. The Mn $2p_{3/2}$ peak measured from the manganese-molybdenum oxides appeared at 642.3 eV and Mn 3s multiplet splitting was 4.8 eV, corresponding to the Mn^{4+} state [25] and the Mo 3d spectrum was composed of a doublet at 231.9 eV and 235.1 eV, which was assigned to Mo $3d_{5/2}$ and Mo $3d_{3/2}$ peaks for the Mo^{6+} state [26]. Thus, manganese and molybdenum in the manganese-molybdenum co-deposits are in the Mn^{4+} and Mo^{6+} states. Hereafter, the deposits containing molybdenum will be referred to as $Mn_{1-x}Mo_xO_{2+x}$.

The potentiodynamic anodic polarisation curves in 0.5 M NaCl at pH 8 and 30 °C for MnO_2 and $Mn_{1-x}Mo_xO_{2+x}$ anodically deposited on IrO_2-coated titanium substrate as a function of molybdenum content in the deposits are shown in Figure 3. The anodic current densities of $Mn_{1-x}Mo_xO_{2+x}$ (x = 0.13 – 0.19) are almost independent of molybdenum content and are lower than that of molybdenum free MnO_2 in the potential region of about 1.24 to 1.6 V (NHE), indicating a lower activity of the three former electrodes than the latter for gas evolution. In the potential range exceeding 1.6 V (NHE), the current densities of the deposits with and without molybdenum are almost the same. On the other hand, $Mn_{1-x}W_xO_{2+x}$ electrodes showed a higher activity than the MnO_2 electrode for gas evolution [20].

Figure 4 shows the oxygen evolution efficiency at 1,000 A m^{-2} in 0.5 M NaCl at pH 8 and 30 °C for anodically deposited MnO_2 and $Mn_{1-x}Mo_xO_{2+x}$ as a function of concentration of Na_2MoO_4 in the baths. The fraction of molybdenum in $Mn_{1-x}Mo_xO_{2+x}$ is also shown in this figure. It is clear that the efficiency of oxygen evolution on $Mn_{1-x}Mo_xO_{2+x}$ electrodes is much higher than that of the MnO_2 electrode. Measurements of the oxygen evolution efficiency were repeated three or four times. As described elsewhere [18, 20, 21], the accuracy of chlorine analysis by the iodimetric titration is significantly high and the detection limit in this experiment is 0.1 g m^{-3} of chlorine (2.72×10^2 C m^{-3}). Thus, if total amounts of chlorine and hypochlorite are below the detectable limit, the oxygen evolution efficiency is taken as 100% . As can be seen from Figure 4, 100% oxygen evolution efficiency is seen in the deposit with 13 mol% molybdenum (0.003 M Na_2MoO_4), and 99.9% efficiency for the deposits with 15 (0.005 M Na_2MoO_4), 19 (0.02 M Na_2MoO_4) and 21 mol% molybdenum (0.04 M Na_2MoO_4) and 99.0% efficiency for the deposit with 22 mol% molybdenum (0.1 M Na_2MoO_4). This is the first time that such a high oxygen evolution efficiency, more than 99.9% , has been

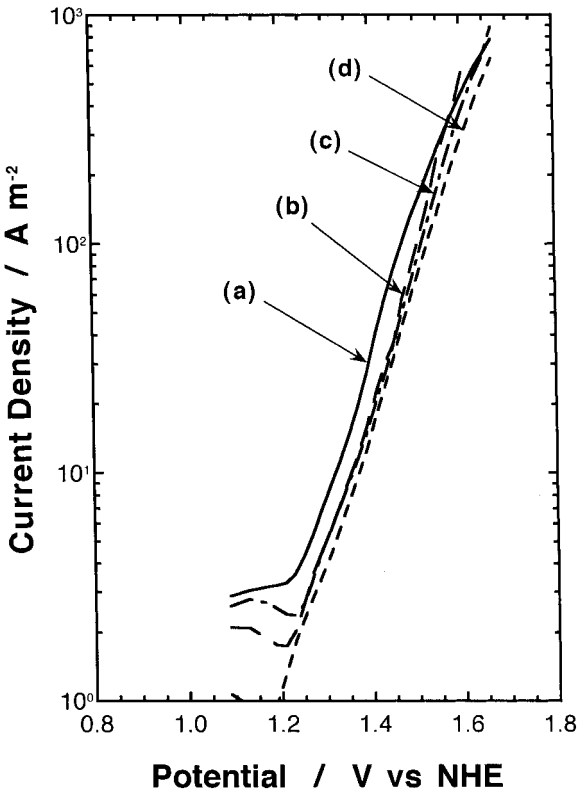

Fig. 3. Potentiodynamic anodic polarisation curves in 0.5 M NaCl at pH 8 and 30 °C for anodically deposited MnO_2 and $Mn_{1-x}Mo_xO_{2+x}$ on IrO_2-coated titanium substrates prepared at 600 A m^{-2} from the baths containing 0.2 M $MnSO_4$ and 0–0.02 M Na_2MoO_4 at pH 0.5 and 90 °C. (a) 0 M (x = 0), (b) 0.005 M (x = 0.15), (c) 0.003 M (x = 0.13) and (d) 0.02 M (x = 0.19) Na_2MoO_4.

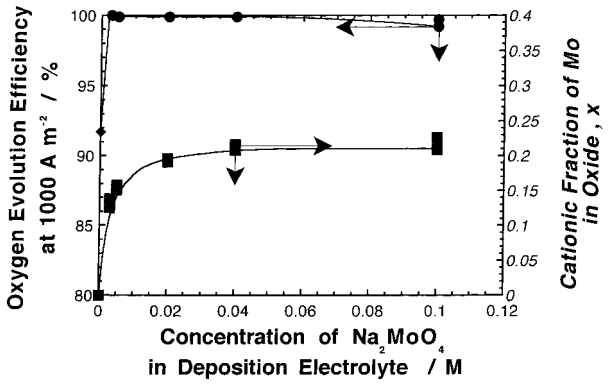

Fig. 4. Oxygen evolution efficiency measured at 1,000 A m^{-2} in 0.5 M NaCl at pH 8 and 30 °C for anodically deposited MnO_2 and $Mn_{1-x}Mo_xO_{2+x}$ on IrO_2-coated titanium substrates prepared at 600 A m^{-2} from the baths containing 0.2 M $MnSO_4$ and 0–0.1 M Na_2MoO_4 at pH 0.5 and 90 °C for 10 min (◆) and 30 min (●). The fraction of Mo^{6+}, x, in $Mn_{1-x}Mo_xO_{2+x}$ (■) is also shown.

achieved at 1,000 A m^{-2} in 0.5 M NaCl at pH 8. The oxygen evolution efficiencies so far reported are 99.6% on an anodically deposited $Mn_{1-x}W_xO_{2+x}/IrO_2/Ti$ at 200 A m^{-2} [20], 99% on an anodically deposited MnOx/RuO_2/Ti [13], 92% on a thermally decomposed (Mn-W)Ox/IrO_2/Ti at 200 A m^{-2} [17] and 90% on anodically deposited MnOx/RuO_2/Ti at 1,000–4,000 A m^{-2} [15].

The durability of these electrodes for oxygen evolution was examined in 0.5 M NaCl at pH 12 and 30 °C. Even in the solution of pH 12, the oxygen evolution efficiency at a constant current density of 1,000 A m^{-2} was almost the same as that in the solution of pH 8 shown in Figure 4; that is, 100% efficiency for oxygen evolution is also attained on the electrode. It can, therefore, be said that the $Mn_{0.87}Mo_{0.13}O_{2.13}$ is a candidate material as the anode for seawater electrolysis without releasing chlorine. Figure 5 shows the galvanostatic anodic polarisation curves in 0.5 M NaCl at pH 12 and 30 °C for MnO_2 and $Mn_{0.87}Mo_{0.13}O_{2.13}$ anodically deposited on the IrO_2-coated titanium substrate. The polarisation curves of these electrodes are composed of two Tafel regions. The resulting Tafel line displays a change in slope at a current density around 1,000 A m^{-2} or near an overpotential of 1.3 V. In the low Tafel region, the anodic current density of the $Mn_{0.87}Mo_{0.13}O_{2.13}$ electrode is lower than that of MnO_2 electrode, similarly to the solution at pH 8 (Figure 3), but in the high Tafel region the current densities for both electrodes are almost the same. Two Tafel regions were also reported for the $Mn_{1-x}W_xO_{2+x}$ coatings whose anodic current density is higher than that of the MnO_2 electrode, particularly at high current densities [20]. Nevertheless, $Mn_{0.87}Mo_{0.13}O_{2.13}$ is capable of evolving oxygen from sodium chloride solutions with 100% efficiency. It can, therefore, be said that molybdenum addition to manganese oxide is more effective in enhancing the selectivity of oxygen evolution from chloride solutions than tungsten addition.

Such a high efficiency of oxygen evolution for this electrode is maintained at high electrolysis current densities in 0.5 M NaCl at pH 12. Figure 6 shows the change in the oxygen evolution efficiency and polarisation potential on the $Mn_{0.87}Mo_{0.13}O_{2.13}$ electrode as a function of current density in 0.5 M NaCl at pH 12 and 30 °C. The oxygen evolution efficiency on the MnO_2 electrode is also shown for comparison. The efficiency for the $Mn_{0.87}Mo_{0.13}O_{2.13}$ electrode is remarkably higher than that for the MnO_2 electrode. Furthermore, for the $Mn_{0.87}Mo_{0.13}O_{2.13}$ electrode almost no change in the efficiency exceeding 99.9% is observed with increase in current density from 100 to 10,000 A m^{-2}. Similar results were obtained in solution of pH 8. On the other hand, the efficiency of the MnO_2 electrode at 100 A m^{-2} is as low as 88.3% and exhibits a 5% decrease with increase in current density from 100 to 1,000 A m^{-2}. In the case of the MnO_2 electrode, because violent oxygen

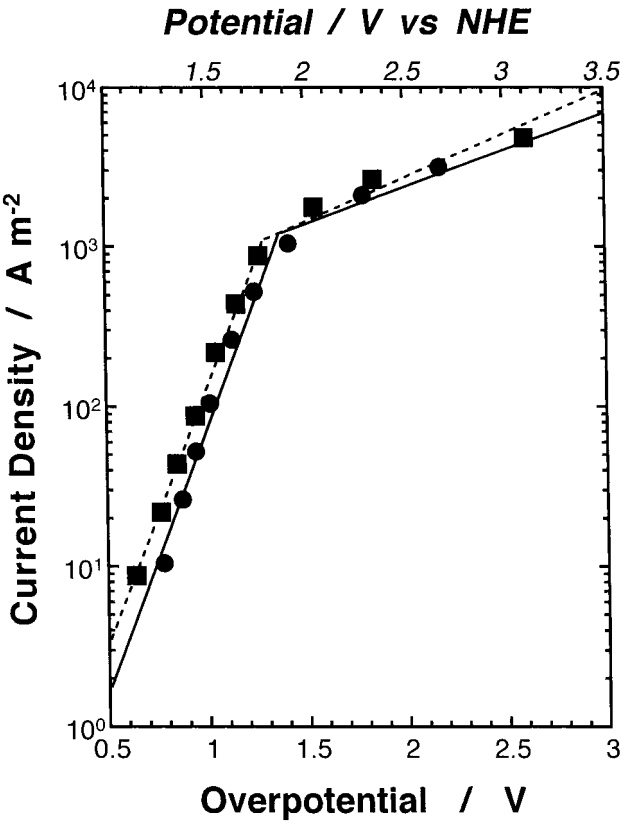

Fig. 5. Galvanostatic anodic polarisation curves in 0.5 M NaCl at pH 12 and 30 °C for MnO_2 (■) and $Mn_{0.87}Mo_{0.13}O_{2.13}$ (●) anodically deposited on IrO_2-coated titanium substrates.

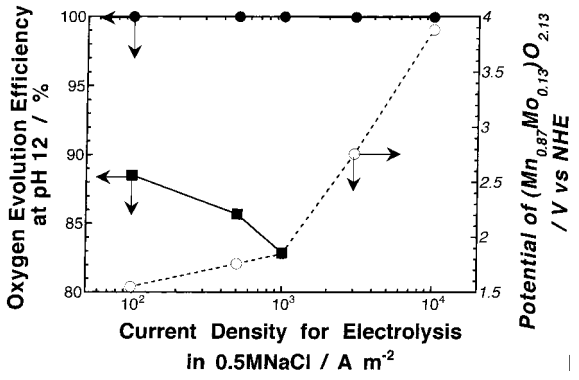

Fig. 6. Oxygen evolution efficiency measured at different current densities of electrolysis in 0.5 M NaCl at pH 12 and 30 °C for anodically deposited MnO_2 (■) and $Mn_{0.87}Mo_{0.13}O_{2.13}$ (●) anodically deposited on IrO_2-coated titanium substrates. The polarisation potential on the $Mn_{0.87}Mo_{0.13}O_{2.13}$ (○) is also shown.

evolution at high current densities above 3,000 A m^{-2} gave rise to peeling of the deposit from the IrO_2-coated titanium substrate, no measurement of the oxygen evolution efficiency was done at high current densities, indicating poor adhesiveness of the deposit without molybdenum. It can, therefore, be said that the addition of molybdenum to the deposits is effective in improving not only the electrocatalytic activity for oxygen evolution but also the adhesiveness of the deposits.

Since the total anodic current density is the sum of the current densities of oxygen and chlorine evolution, the current density-potential curves of oxygen and chlorine evolution for an MnO_2 electrode were obtained from the efficiency data for oxygen evolution. Results are shown in Figure 7. Because the oxygen evolution efficiency for the $Mn_{0.87}Mo_{0.13}O_{2.13}$ electrode is 100% up to a current density of 1,000 A m^{-2}, the current density for chlorine evolution is almost four orders of magnitude lower than the oxygen evolution current density. It is clear from this figure that the current densities for oxygen evolution for $Mn_{0.87}Mo_{0.13}O_{2.13}$ at given potentials are slightly lower than those of the MnO_2 electrode and, interestingly, the current densities for chlorine evolution for $Mn_{0.87}Mo_{0.13}O_{2.13}$ should be more than three orders of magnitude lower than those for MnO_2. Therefore, the addition of molybdenum to the deposits suppresses the electrocatalytic activity exclusively for chlorine evolution, although it slightly reduces the activity for oxygen evolution, resulting in the ability to evolve oxygen from sodium chloride solutions with 100% efficiency.

The durability of the anodically deposited $Mn_{0.87}Mo_{0.13}O_{2.13}$ electrode for oxygen evolution in 0.5 M NaCl, 30 °C at pH 8 and 12 is shown in Figure 8. The electrode retained its high efficiency for oxygen evolution exceeding 96% for 2,800 h in the solution of pH 8 and 99.5% for 1,000 h in the solution of pH 12 at 1,000 A m^{-2}. Similar durability was obtained for the $Mn_{1-x}W_xO_{2+x}$ electrodes under equivalent conditions [27]. Therefore, $Mn_{1-x}Mo_xO_{2+x}$, as well as $Mn_{1-x}W_xO_{2+x}$, are good candidate materials for the oxygen evolving anode in seawater electrolysis. In long term operation, the oxygen evolution efficiency is gradually reduced. This is possibly due to dissolution of molybdenum from the deposits. The characterisation of the deposits is now in progress.

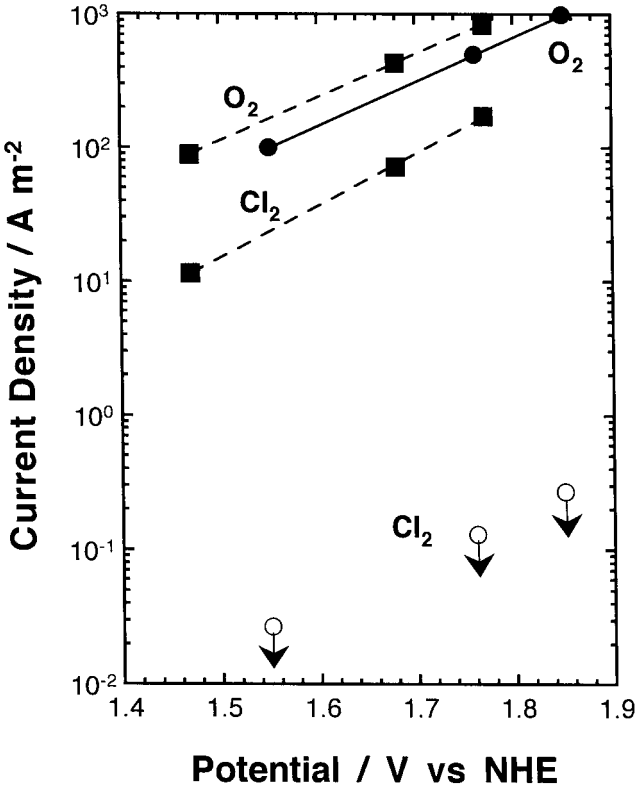

Fig. 7. Current density-potential curves of oxygen and chlorine evolution for MnO_2 (■) and oxygen evolution for $Mn_{0.87}Mo_{0.13}O_{2.13}$ (●) electrodes anodically deposited on IrO_2-coated titanium substrates. ○ with arrow shows the detectable limit in this experiment.

4. Conclusions

The anodic deposition has been applied to the preparation of manganese and manganese-molybdenum oxide oxygen electrodes which avoid chlorine evolution in the electrolysis of seawater. Their oxygen evolution efficiency was examined at a current density of 1,000 A m^{-2} in a 0.5 M NaCl solution at 30 °C and pH 8 or 12. The following conclusions can be drawn.

1. Manganese-molybdenum deposits consist of a single γ-MnO_2 type phase, and manganese and molybde-

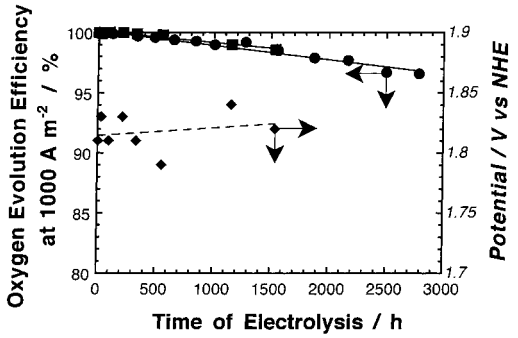

Fig. 8. Change in the oxygen evolution efficiency measured at 1,000 A m^{-2} in 0.5 M NaCl, 30 °C at pH 8 (●) and 12 (■) for anodically deposited $Mn_{0.87}Mo_{0.13}O_{2.13}$ electrode with time. The polarisation potential on the $Mn_{0.87}Mo_{0.13}O_{2.13}$ at pH 12 (◆) is also shown.

num in the deposits are in the Mn^{4+} and Mo^{6+} states.

2. The addition of molybdenum to the γ-MnO_2 improves the efficiency for oxygen evolution remarkably. The efficiency of the deposits containing 13–21 mol% molybdenum is more than 99.9% at 1,000 A m^{-2} at pH 8. 100% efficiency is attained at 1,000 A m^{-2} for a deposit with 13 mol% molybdenum ($Mn_{0.87}Mo_{0.13}O_{2.13}$). Even at higher current density of 10,000 A m^{-2} in solutions of pH 8 and 12, 99.9% oxygen evolution efficiency is obtained with the $Mn_{0.87}Mo_{0.13}O_{2.13}$ electrode.
3. The addition of molybdenum is also effective in improving durability in electrolysis. $Mn_{0.87}Mo_{0.13}O_{2.13}$ electrode shows oxygen evolution efficiency of 98.5% for over 1,500 h in the solution of pH 12 and 96.5% for over 2,800 h in the solution of pH 8 with continuous electrolysis at 1,000 A m^{-2}.
4. The improvement of both the oxygen evolution efficiency and durability by the addition of molybdenum is due to the suppression of the activity for chlorine evolution below the detectable limit of chlorine, though the molybdenum addition slightly decreases the activity for oxygen evolution.

Acknowledgment

This work was supported in part by a Grant-in Aid for Scientific Research (A-2 07405032, C-2 09650778) from The Ministry of Education, Science, Sports and Culture, Japan.

References

1. K. Hashimoto, *Materia Japan* **33** (1994) 559.
2. K. Hashimoto, *Mater. Sci. Eng.* **A179/A180** (1994) 27.
3. K. Hashimoto, *Proc Advanced Materials '93* (edited by R. Yamamoto, E. Furubayashi, Y. Doi and B. Liu) **18A** Elsevier Science, (1994), p. 35.
4. K. Hashimoto, H. Habazaki and E. Akiyama, *J. Soc. Mat. Sci. Japan* **45** (1966) 1067.
5. K. Hashimoto, E. Akiyama, H. Habazaki, A. Kawashima, K. Shimamura, M. Komori and K. Kumagai, 'Zairyo to Kankyo' *Corros. Eng.* **45** (1996) 614.
6. K. Hashimoto, E. Akiyama, H. Habazaki, A. Kawashima, M. Komori, K. Shimamura and K. Kumagai, *Sci. Rep. Res. Inst. Tohoku University* **A43** (1997) 153.
7. A.F. Adamson, B.J. Level and W.F. Stones, *J. Appl. Chem.* **13** (1963) 483.
8. J.E. Bennett, *Chem. Eng. Prog.* **70** (1974) 60.
9. N. Kumagai, Y. Samata, S. Jikihara, A. Kawashima, K. Asami and K. Hashimoto, *Mater. Sci. Engng.* **99** (1988) 489.
10. M. Morita, C. Iwakura and H. Tamura, *Electrochim. Acta* **22** (1977) 325.
11. M. Morita, C. Iwakura and H. Tamura, *Electrochim. Acta* **23** (1978) 331.
12. M. Morita, C. Iwakura and H. Tamura, *Electrochim. Acta* **24** (1979) 357.
13. J.E. Bennett, *World Hydrogen Energy Conf.* 1978, p. 291.
14. J.E. Bennett, *Int. J. Hydrogen Energy* **5** (1980) 401.
15. M. Hiroi, M. Muroya, E. Tada and S. Ogawa, *DENKI KAGAKU* **57** (1989) 837.
16. M. Hiroi, Y. Takemoto, M. Muroya and E. Tada, *DENKI KAGAKU* **58** (1990) 184.
17. K. Izumiya, E. Akiyama, H. Habazaki, N. Kumagai, A. Kawashima and K. Hashimoto, *Mater. Trans. JIM* **38** (1997) 899.
18. K. Izumiya, E. Akiyama, A. Kawashima, K. Asami and K. Hashimoto, *J. Appl. Electrochem.* **27** (1997) 1362.
19. K. Izumiya, E. Akiyama, H. Habazaki, N. Kumagai, A. Kawashima and K. Hashimoto, *Mater. Trans. JIM* **39** (1998) 308.
20. K. Izumiya, E. Akiyama, H. Habazaki, N. Kumagai, A. Kawashima and K. Hashimoto, *Electrochimica Acta* **43** (1998) 3303.
21. K. Izumiya, Doctor thesis, Tohoku University (1998).
22. K. Asami, *J. Electron Spectrosc.* **9** (1976) 469.
23. K. Asami and K. Hashimoto, *Corros. Sci.* **17** (1977) 559.
24. N. Kumagai, Y. Samata, A. Kawashima, K. Asami and K. Hashimoto, *J. Appl. Electrochem.* **17** (1987) 347.
25. M. Oku, K. Hirokawa, and S. Ikeda, *J. Electron Spectroc.* **7** (1975) 465.
26. K.S. Kim and N. Wignograd, *Surface Sci.* **43** (1974) 625.
27. K. Izumiya, K. Fujimura, E. Akiyama, H. Habazaki, A. Kawashima and K. Hashimoto, *Proc of EUROMAT '98 Conference on Materials in Oceanic Environment*, The Federation of European Materials Science Vol. 1 (1998) p. 37.